# Decay dynamics of $H_2O(^1B_1)$: full characterization of OH product state distribution

Klaus Mikulecky, Karl-Heinz Gericke and Franz Josef Comes

*Institut für Physikalische und Theoretische Chemie der Johann Wolfgang Goethe-Universität, Niederurseler Hang, W-6000 Frankfurt am Main 50, Germany*

Received 23 January 1991; in final form 30 April 1991

$H_2O$ was excited to the lowest electronic excited state, $^1B_1$, at 157.6 nm and the OH product state distribution was completely analyzed by special laser-induced-fluorescence (LIF) experiments probing the fragment distribution by the transitions ($v' = 0, 1 \leftarrow v''$). The OH rotational excitation is relatively low and can be described by a temperature parameter of $\approx 500$ K independently of the OH vibrational excitation. This is in accordance with former measurements as well as with theoretical calculations. No selective population of the electronic fine-structure levels was observed which is in agreement with the expectations for a room-temperature experiment. The observed magnitude of the vibrational excitation ($P(v''=0): P(v''=1): P(v''=2): P(v''=3): P(v''=4) = 59.2:33.1:6.1:1.4:0.2$) is smaller than the one calculated. The calculations predicted the $v'' = 6$ level to be populated, whereas in the experiment, transitions probing the $v'' = 5$ state were not observed.

## 1. Introduction

The present investigation of the photodissociation dynamics of water in its first absorption band refers to the following process [1,2]:

$$H_2O(^1A_1) + h\nu(157.6\,\text{nm}) \rightarrow H_2O(^1B_1)$$
$$\rightarrow OH(^2\Pi, v, J) + H(^2S)\,.$$

OH is formed in its electronic ground state exclusively. This process has been investigated in detail by Andresen et al. [3].

The photodissociation of $H_2O$ is a simple, direct photochemical reaction. The number of involved electrons is sufficiently small to perform calculations on the potential surface [4], so that a direct comparison between theoretical predictions and experimental results becomes possible. The photodissociation can be treated as a half-collision process. The product energy distribution and fragment alignment are accessible by calculations. The system may serve as a model for direct photodissociation processes in which the ground-state wavefunction determines the rotational and electronic fine-structure product state distribution. Investigations of the photodissociation of water apart from the quoted paper [3] have dealt with the second absorption band and the production of OH in the electronically excited state, $A\,^2\Sigma^+$, and the ground state $^2\Pi$ [5].

The results in the case of the photodissociation of water in its first absorption band can be summarized as follows: The photolysis of water at 157.6 nm produces OH with low rotational excitation. The observed rotational-state distributions correspond to a temperature of 930 K in $v'' = 0$ and 840 K in $v'' = 1$. The vibrational states $v'' = 0$ and $v'' = 1$ were shown to be almost equally populated with a ratio of 1:0.95. The $v'' = 2$ population could not be determined precisely because of the predissociative A state of OH. The rotational temperature in $v'' = 2$ was estimated to be similar to $v'' = 0$ and 1.

Clearly different results were obtained when the parent molecules were cooled down in a nozzle beam. The rotational temperature of the OH product drops to 210 K or 475 K, respectively, for the two $\Lambda$ sublevels of OH. The $\Lambda$ sublevels show a different population when jet-cooled water is photolyzed. This effect is not observable in the static gas. This preferred formation of OH in the $\Pi(A'')$ state results from conservation of symmetry. The $\tilde{A}\,^1B_1$ state of the dis-



0009-2614/91/$ 03.50 

sociating $H_2O$ molecule is antisymmetric, the hydrogen atom in a $^2S_{1/2}$ state is symmetric; thus the OH must be formed in the antisymmetric $\Pi(A'')$ state to conserve symmetry. At room temperature, this is not so evident because of thermal rotation of the parent, so an equal distribution results.

Photodissociation of $H_2O$ was investigated as well at a wavelength of 193 nm, despite the very small absorption cross section [6,7]. Measurements in static gas show a rotational temperature of 400 K in $v''=0$ which is the only populated vibrational state. The rotational temperature decreases to 330 K when measured in a nozzle beam, similarly to the 157.6 nm photolysis. The preferential formation of OH $\Pi(A'')$ is observed as well.

Furthermore, state-to-state experiments were performed in which a single rotational–vibrational state of $H_2O$ was prepared by infrared excitation before photolysis at 193 nm. The experimental results were compared to results from calculations [8,9]. It was found that after a state-selective excitation of $H_2O$, the rotational distribution of OH can by no means be described by a Boltzmann distribution. Further, there is a strong preference for the upper component of the $\Lambda$ sublevels. The correlation between theory and experiment is remarkably good.

With respect to these experimental results a theoretical model was developed [10–12]. It could be shown that the product state distribution from the photolysis of water can be described by the Franck–Condon limit, as far as rotation and electronic fine structure like spin–orbit and $\Lambda$ states are concerned. However, regarding the vibration, there is a strong coupling between the OH product states and the $H_2O$ initial states, i.e. final state interaction is responsible for OH vibration. The calculations predicted high vibrationally excited OH photofragments up to $v''=6$. The rotational excitation was expected to be rather low. Guo and Murrell [11,12] obtained the maximum of the rotational distribution at $J''=1$.

The aim of the present investigation was to measure the recoil velocity of the fragments and the complete rotational and vibrational distribution of OH in all populated vibrational states, that is from $v''=0$ to $v''=4$. Due to predissociation of OH (A), the vibrational levels higher than $v'=1$ are not accessible by direct "diagonal" $\Delta v=0$ excitation. It is necessary to excite OH from all $v''$ states to $v'=0$ and 1 only, so $\Delta v=0, -1, -2$ and $-3$ bands had to be observed.

## 2. Experimental

State-specific analysis of nascent OH ($^2\Pi_\Omega$, $v$, $J$) products in the photodissociation of $H_2O$ at 157 nm has been performed by the pump and probe technique. For photolysis, we used a $F_2$ excimer laser (Lambda Physik EMG 201) with an average pulse energy of about 5 mJ. The VUV beam was slightly focused into the gas cell by a LiF lens, $f\approx 30$ cm. An excimer-pumped dye laser generated the probe beam. It was focused weakly and counterpropagated the photolysis beam collinearly. The lasers were triggered by a delay generator at 10 Hz. The delay between the pump and probe pulses was 20 ns. The measurements were carried out in a flow cell at a total pressure of 0.7 Pa, determined by a MKS Baratron capacitance gauge. Thus, the products were probed under collision-free conditions. Since wavelengths from 306 to 520 nm had to be covered, it was necessary to double the frequency of the dye-laser radiation when probing the $\Delta v=0$ bands of OH. Frequency doubling was achieved by an autotracking system with a KDP crystal (inrad). Wavelengths longer than 340 nm were generated directly. Table 1 gives the investigated bands and the necessary laser dyes.

The bandwidth of the dye-laser radiation was about 0.4 $cm^{-1}$. For line profile measurements, it is possible to attach an airspaced étalon to the laser oscil-

Table 1
Observed transitions and laser dyes in the OH $A\,^2\Sigma^+(v', J')$–$X\,^2\Pi(v'', J'')$ system for the analysis of the product state population of OH fragments

| $v'$ | $v''$ | $\lambda$ (nm) | Dye |
|---|---|---|---|
| 0 | 0 | 306–318 | SR 101/DCM (SHG) |
| 1 | 1 | | |
| 0 | 1 | 343–357 | DMQ |
| 1 | 2 | | |
| 0 | 2 | 388–403 | PBBO |
| 1 | 3 | | |
| 0 | 3 | 440–459 | coumarin 2 |
| 1 | 4 | | |
| 0 | 4 | ≈520 | coumarin 334 |
| 1 | 5 | | |

lator. This reduces the bandwidth to about 0.05 $cm^{-1}$.

The pulse energy was kept sufficiently low to prevent saturation effects. The linear dependence of the signal intensity on the probe laser power was tested for each $(v', v'')$ band by decreasing the laser power with a filter of known transmission. We probed the $\Delta v=0$ band with about 10 μJ, the $\Delta v\neq 0$ bands with up to 5 mJ because of the lower Einstein $B$ coefficients. The $\Delta v=4$ band was not observed even at pulse energies higher than 10 mJ.

The LIF signal was observed with a photomultiplier through a spectral filter with peak transmission at 310 nm. This filter allowed equal transmission for the $v'=0$ to $v''=0$ and $v'=1$ to $v''=1$ fluorescence but no transmission for the $v'=1$ to $v''=0$ transition around 280 nm. After an excitation to $v'=1$, 25% of the total fluorescence intensity is radiated from this $v'=1$ to $v''=0$ transition. This cut-off by our filter was considered in the determination of the product state distribution.

The fluorescence signal was normalized to the pulse energies of the pump and probe lasers. The photomultiplier and reference diode outputs were registered by a boxcar integrator system and recorded by a computer (PC/AT 386) after A/D conversion.

## 3. Results

### 3.1. Rotational-vibrational state distribution

The OH transitions were assigned following the spectral tables of Dieke and Crosswhite [13] and Coxon [14]. For the $\Delta v<0$ bands, the transitions had to be calculated from the OH energy levels. Fig. 1 shows a scan in the region from 395 to 400.8 nm and corresponds to a $A\,^2\Sigma(v'=0, 1)\leftarrow X\,^2\Pi(v''=2, 3)$ transition. Since the transitions were not saturated, the line intensities were converted to populations by using transition probabilities. The transition probability for a transition $A\,^2\Sigma^+(v', J')\leftarrow X\,^2\Pi(v'', J'')$ consists of two factors, the Einstein $B$ coefficient for the vibrational transition, $B(v', v'')$, and the Hönl–London factor for the rotational transition, $S(J', J'')$.

The total Einstein $B(v', v'', J', J'')$ coefficient for a rotational-vibrational transition from $v'', J''(N'')$ to $v', J'(N')$ is given by

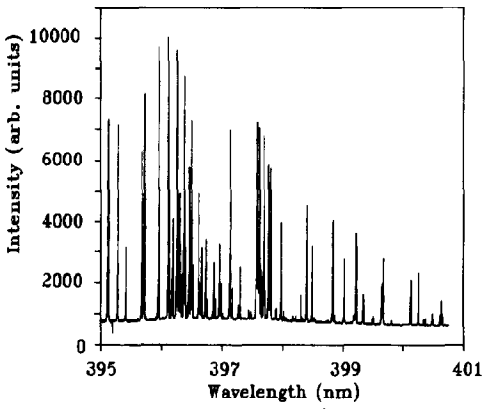


Fig. 1. LIF spectrum of OH from 395 to 400.8 nm showing the $v'=0$–$v''=2$ and $v'=1$–$v''=3$ transitions.

$$B(v', v'', J', J'') = \frac{8\pi^3}{3h^2c_0}\frac{p(v', v'', N', N'')S(J', J'')}{2J''+1}.$$

Combined with the photolysis and probe laser powers $W_{ph}$ and $W_{pr}$, the Einstein $B$ coefficients normalize the line intensity $I(v'', J'')$ to a population:

$$P(v'', J'') = \frac{I(v'', J'')}{B(v', v'', J', J'')W_{ph}W_{pr}}.$$

The vibrational Einstein $B$ coefficients are tabulated very differently in the literature, as may be seen from the summary in table 2.

We decided to use our own transition probabilities (table 3) because they are a complete set for all transitions we observed. Different transition probabilities are the main cause of the uncertainty in determining population numbers. Thus, the error bars in fig. 4 are not a result of the measurements, but were derived from a data evaluation with the transition probabilities of Dimpfl and Kinsey [15]. The Hönl–London factors for the rotation were taken from ref. [13] and the populations $P(v'', J'')$ were calculated with the equation given above.

To determine the rotational temperature, we plotted $\ln[P(v'', J'')/(2J''+1)]$ versus $E(v'', J'')$. This is a Boltzmann plot, originating from the Boltzmann distribution law:

$$P(v'', J'') = (2J''+1)Q^{-1}(v'')P(v'') \times \exp[-\Delta E(v'', J'')/kT(v'')].$$

Table 2
Comparison of relative Einstein $B$ coefficients normalized to $B(v'=0, v''=0)=1000$

| Transition ($v'-v''$) | This work | Ref. [13] | Ref. [15] | Ref. [16] | Ref. [17] |
|---|---|---|---|---|---|
| 0–0 | 1000 | 1000 | 1000 | 1000 | 1000 |
| 1–1 | 597 | 700 | 606 | – | 601 |
| 0–1 | 14 | 5 | 4.3 | – | – |
| 1–2 | 21 | 13 | 3.3 | – | – |
| 0–2 | 0.32 | – | 0.6 | 0.08 | – |
| 1–3 | 1 | – | 3.1 | 0.6 | – |
| 0–3 | 0.005 | – | 0.08 | – | – |
| 1–4 | 0.12 | – | – | – | – |

Table 3
Population of the vibrational levels of OH

| | $P(v'')$ | | | | | |
|---|---|---|---|---|---|---|
| | $v''=0$ | $v''=1$ | $v''=2$ | $v''=3$ | $v''=4$ | $v''=5$ |
| this work | 59.2 | 33.1 | 6.1 | 1.4 | 0.2 | <0.02 |
| ref. [15] | 56.3 | 30.1 | 11.1 | 1.7 | – | – |
| ref. [11] [a] | 29 | 26 | 18 | 12 | 8 | 7 |

[a] Theoretical values.

$Q$ means the partition function, $\Delta E(v'', J'')$ the rotational energy with respect to the lowest rotational state in the specific $v''$ level. The Boltzmann plot yields a relative value for $P(v'')$ when the line is extrapolated versus $\Delta E(v'', J'')=0$. The influence of the partition function is of minor importance here because it is nearly equal for all vibrational states under investigation.

In general, the varying power of the probe laser, as well as a changing beam diameter over a wide wavelength range, presents an essential experimental problem in the evaluation of the vibrational populations. However, in the present case of OH detection, a pair of OH vibrational bands with the same $\Delta v$ ($0\leftarrow v''$ and $1\leftarrow v''+1$) is accessible within a single narrow scan (see table 1). Thus, it is possible to derive a ratio between the two probed $v''$ levels. We determined the ratios $P(v''=0)/P(v''=1)$, $P(v''=1)/P(v''=2)$, $P(v''=2)/P(v''=3)$ and $P(v''=3)/P(v''=4)$. The overlap between them makes it possible to compare the populations in the vibrational states directly without being disturbed by difficulties arising from comparing the probe laser powers over a wide spectral range.

All Boltzmann plots for $v''<4$ show linearity. As an example, the rotational distribution of the $v''=3$ state is shown in fig. 2a. Only in $v''=4$ are the higher rotational levels populated stronger than is expected in a thermal distribution (fig. 2b). However, the de-

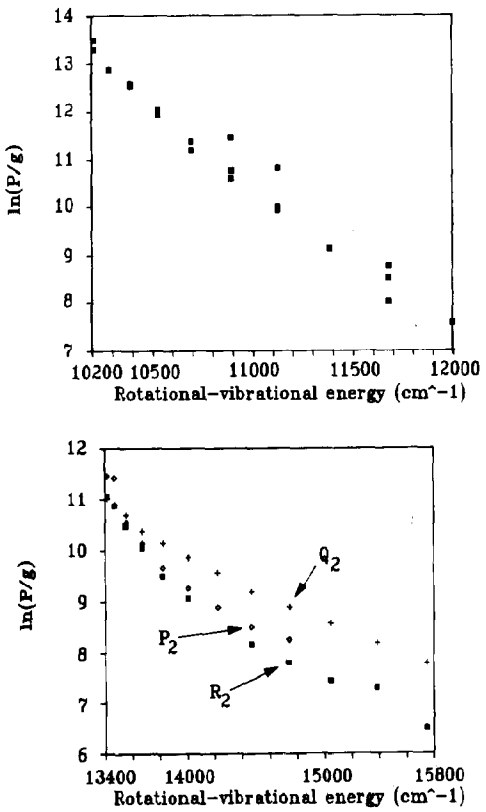


Fig. 2. (a) Boltzmann plot of the rotational state distribution in $v''=3$ derived from the $A\,^2\Sigma(v'=0)\leftarrow X\,^2\Pi(v''=3)$ transition. (b) Boltzmann plot of the rotational state distribution in $v''=4$ derived from the $A\,^2\Sigma(v'=1)\leftarrow X\,^2\Pi(v''=4)$ transition.

Table 4
Observed rotational temperature parameter $T(v'')$, in K

| | $v''=0$ | $v''=1$ | $v''=2$ | $v''=3$ | $v''=4$ |
|---|---|---|---|---|---|
| $v'=0$ | 620 | 460 | 380 | 460 | - |
| $v'=1$ | - | 440 | 500 | 550 | 950 |
| mean | 620 | 450 | 440 | 500 | 949 |

viation from linearity is less than 10% so that a linear extrapolation describes the overall distribution fairly well. The observed rotational temperatures of the vibrational states $v''=0$ to $v''=4$ are summarized in table 4.

### 3.2. Spin–orbit and Λ-state distribution

We neither found a preferential production of OH in one of its spin-orbit states $^2\Pi_{1/2}$ and $^2\Pi_{3/2}$, nor in one of the $\Lambda$ sublevels $\Pi(A')$ and $\Pi(A'')$. This is not surprising, because it was shown before, that those effects occur only when the measurements are performed in a nozzle beam.

### 3.3. Fragment recoil velocity

We have determined the photofragment velocity by high-resolution measurements of the lines of the $Q_1(2)$ and $Q_1(3)$ ($v'=0$ to $v''=0$) transitions (fig. 3). We found a Doppler width of 0.15 $cm^{-1}$ which corresponds to a fragment velocity of about 1380 m $s^{-1}$. For a fragment in the $J''=3$, $v''=0$ state, the recoil velocity should be 1310 m $s^{-1}$ due to conservation of energy and linear momentum. Thus, there is a very good agreement with the experimental data.

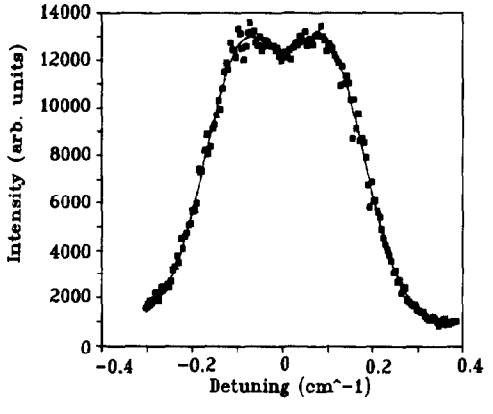


Fig. 3. High-resolution scan of the $Q_1(2)$ ($v'=0$, $v''=0$) transition (squares) and Doppler fit (solid line).

### 3.4. Alignment effects

Correlation between the transition dipole moment of the parent, $\mu(H_2O)$, and the product recoil velocity as well as a correlation between the translational and rotational motion of the fragment can be extracted from the shape of the spectral lines [7]. The intensity of the transitions is only affected by the alignment of the rotational vector of the product and the dipole moment of the parent. Since we used unpolarized laser beams and determined the population number of each rotational state by averaging over the P, Q and R transitions, a maximum alignment will influence the measurement by only 15%. Furthermore, a significant alignment was only observed for jet-cooled parents [3], and thus any influence of an alignment in the determination of the OH product state distribution in the photodissociation of $H_2O$ at room temperature can be neglected.

## 4. Discussion

The experimental results of this work approximately resemble former results [3]. The slightly higher rotational temperature and population of the $v''=1$ states may be a result of incomplete saturation of the OH (A←X) transitions or wavelength dependence of the detection of fluorescence light. In the present work, any saturation of the LIF signal was avoided and the transmission of the fluorescence filter was taken into account. With the results obtained, we calculated the partition of the total energy to the degrees of freedom of our system. The photolysis energy (157.6 nm) is 63450 $cm^{-1}$ (759 kJ $mol^{-1}$) and the internal energy of $H_2O$ at 300 K is 3.7 kJ $mol^{-1}$. The dissociation of $H_2O$ needs 493.65 kJ $mol^{-1}$. The rotational energy of the photofragments is

$$E_{\mathrm{rot,total}} = R \sum_{v=0}^{4} P(v) T_{\mathrm{rot}}(v) \quad = 4.6\ \mathrm{kJ\ mol^{-1}},$$

and the vibrational energy is

$$E_{\text{vib,total}} = \sum_{v=0}^{4} P(v)E(v) = 21.3 \text{ kJ mol}^{-1} .$$

Thus, 243.15 kJ $\text{mol}^{-1}$ are left which are released as translational energy of the photofragments, and the mean velocity of the products is

$$\langle v_{\text{OH}} \rangle = 1260 \text{ m s}^{-1}, \quad \langle v_{\text{H}} \rangle = 21400 \text{ m s}^{-1} .$$

The photodissociation of water is regarded as a model system for a direct photodissociation, i.e. a reaction that occurs on a single repulsive potential surface. The Franck–Condon limit is assumed to be valid as far as rotational excitation and electronic fine-structure distribution (spin–orbit and $\Lambda$ components) are concerned and the rotational eigenfunctions of the product molecule are given as a projection of the parent-molecule eigenfunctions. The product state distribution $P(\lambda, T)$ depends on the parent-molecule state distribution $\rho_i(T)$ and the state-to-state cross section $\sigma_{\text{if}}(\lambda)$:

$$P(\lambda, T) = \sum_i \rho_i(T)\sigma_{\text{if}}(\lambda) ,$$

with

$$\rho_i(T) = (2J_i + 1) \exp(\Delta E_i / RT) ,$$

and

$$\sigma_{\text{if}}(\lambda) \sim \nu \left| \int \Psi_i \Psi_f \, d\tau \right|^2 .$$

If there is a strong dependence of the product states on the initial states, it is not to be expected that the OH product exhibits a high rotational temperature if $H_2O$ is photolyzed at room temperature.

The fact that all vibrational states show similar rotational temperatures is a consequence of the decoupling of rotational and vibrational degrees of freedom during the dissociation process. The exception observed for $v'' = 4$ may be due to the H–O–H angle dependence of the $H_2O$ $\tilde{A}\,{}^1B_1$ potential surface. For smaller H–O distances, the potential has a significant minimum at the equilibrium bond angle of 104°. For larger distances, which are related to higher vibrations, this minimum becomes less pronounced. As a consequence, the torque impacting on the dissociating molecules increases, and a higher rotational excitation is obtained. Of course, this is a partial breakdown of the rotation–vibration decoupling.

As far as the electronic fine-structure distribution is concerned we did not observe any indication for a selective population, but this was not expected either. It was already shown that such effects can only by observed when jet-cooled $H_2O$ is photolyzed. Concerning the vibrational distribution, we obtained results that differ to a certain extent from theoretical predictions [18]. Fig. 4 shows the observed OH vibrational distributions at a photolysis wavelength of 157.6 nm. The magnitude of the vibrational excitation we observed is smaller than the one calculated. The calculations predicted $v'' = 6$ to be populated, but we did not even observe the $v'' = 5$ population. Partly, this is effected by the very small Einstein $B$ coefficients for the $^2\Sigma(v=1) \leftarrow {}^2\Pi(v=5)$ transition, but with a small population in $v'' = 4$, we can expect a smaller population in $v'' = 5$. From the noise, we estimate an upper limit of 0.02% for this state. Obviously, completely different transition probabilities would influence the observed vibrational state distribution. However, the use of the former $B$ coefficients [13,15,16] will even intensify the observed trend that the OH vibrational excitation determined in the experiment is lower than the calculated one. The form of the experimental distribution resembles rather the calculated distribution for a photolysis wavelength of 172.2 nm than that of 156.9 nm. We think that a shift of the upper potential surface by $\approx 0.5$ eV could explain the deviation

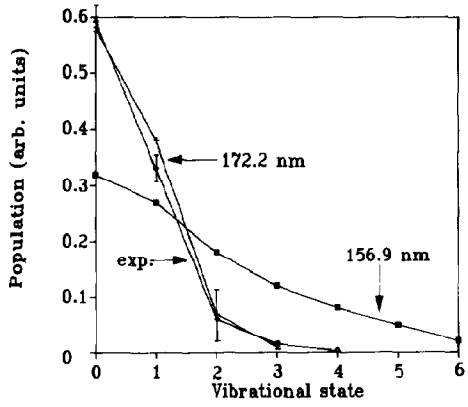


Fig. 4. Theoretically and experimentally obtained vibrational distributions. The error range is calculated by evaluating our data using the transition probabilities of Dimpfl and Kinsey [15], where $v'' = 4$ is not tabulated.

between experimental and theoretical results.

## Acknowledgement

This work has been performed as part of a programme of the Deutsche Forschungsgemeinschaft. We thank Professor V. Staemmler and Dr. R. Schinke for helpful discussions, and Professor P. Rosmus for the calculation of transition probabilities.

## References

[1] K. Watanabe and M. Zelikoff, J. Opt. Soc. Am. 41 (1953) 753.
[2] H. Wang, W.S. Felps and S.P. McGlynn, J. Chem. Phys. 67 (1977) 2614.
[3] P. Andresen, G.S. Ondrey, B. Titze and E.W. Rothe, J. Chem. Phys. 80 (1984) 2548.
[4] V. Staemmler and A. Palma, Chem. Phys. 93 (1985) 63.
[5] J.P. Simons and A.J. Smith, Chem. Phys. Letters 97 (1983) 1;
E. Seger and M. Shapiro, J. Chem. Phys. 77 (1982) 5604, and references therein.
[6] L.C. Lee and M. Suto, Chem. Phys. 110 (1986) 161.
[7] A.U. Grunewald, K.-H. Gericke and F.J. Comes, Chem. Phys. Letters 133 (1987) 501.
[8] P. Andresen, V. Beushausen, D. Häusler and H.W. Lülf, J. Chem. Phys. 83 (1985) 1429.
[9] P. Andresen, D. Häusler and R. Schinke, J. Chem. Phys. 87 (1987) 3949.
[10] P. Andresen and R. Schinke, Molecular photodissociation dynamics, eds. M.N.R. Ashfold and J.E. Baggott (The Royal Society of Chemistry, London, 1987) p. 61.
[11] H. Guo and J.N. Murrell, J. Chem. Soc. Faraday Trans. II 84 (1988) 949.
[12] H. Guo and J.N. Murrell, Mol. Phys. 65 (1988) 821.
[13] G.H. Dieke and H.M. Crosswhite, J. Quant. Spectry Radiative Transfer 2 (1962) 97.
[14] J.A. Coxon, Can. J. Phys. 58 (1980) 933.
[15] W.L. Dimpfl and J.K. Kinsey, J. Quant. Spectry. Radiative Transfer 21 (1979) 233.
[16] C.B. Cleveland, G.M. Jursich, M. Trolier and J.R. Wiesenfeld, J. Chem. Phys. 86 (1987) 3253.
[17] J.R. Chidsey and D.R. Crosley, J. Quant. Spectry. Radiative Transfer 23 (1980) 187.
[18] R. Schinke, in: Collision theory for atoms and molecules, ed. F. Gianturco (Plenum Press, New York, 1988).